

Unveiling quantum complementarity trade-offs in relativistic scenarios

Marcos L. W. Basso  ^{1,*} Ismael L. Paiva  ^{2,†} and Pedro R. Dieguez  ^{3,‡}

¹*Center for Natural and Human Sciences, Federal University of ABC,
Avenida dos Estados 5001, 09210-580, Santo André, São Paulo, Brazil*

²*H. H. Wills Physics Laboratory, University of Bristol,
Tyndall Avenue, Bristol BS8 1TL, United Kingdom*

³*International Centre for Theory of Quantum Technologies,
University of Gdańsk, Jana Bazyńskiego 8, 80-309 Gdańsk, Poland*

Complementarity is a cornerstone of quantum theory, assisting in the analysis and understanding of various quantum phenomena. This concept has even been assumed in theoretical studies in relativistic regimes. Here, we conduct a study of two generalized delayed-choice interferometers traveled by a system with an internal spin. We show how a complete complementarity relation can be indeed applied in these two setups and how the trade-off between the quantities in this relation, namely, path coherence, von Neumann predictability, and entropy of entanglement, is affected by special and general time dilation in an arbitrary spacetime. These modifications originate from Wigner rotations, which couple the spin to the external degrees of freedom of the system and do not rely on the spin acting as a clock. Despite having different complementarity trade-offs, both arrangements have the same interferometric visibility, as we unveil. To give a concrete example, we analyze the Newtonian limit of these results.

I. INTRODUCTION

Bohr's complementarity principle challenges our classical understanding of reality by suggesting that physical systems may have properties that only emerge once the entire physical context for their probing is settled [1, 2]. This idea generates debates to this date [3–7]. To make these discussions more rigorous, various theoretical approaches were introduced to quantify the complementarity principle [8–25]. The most common consists of an inequality involving the sum of interferometric predictability and visibility. However, for several reasons, it has been argued that this inequality fails to capture important aspects of the complementarity principle. For instance, both quantities can simultaneously vanish [26]. This reveals that there is a missing quantity that can be added to the analysis. This quantity, as it turns out, is entanglement [27]. With its addition, one obtains a complete complementarity relation (CCR).

Moreover, visibility may not be a good measure of non-classicality inside the interferometer, with path coherence being better at that [15, 18, 28–30]. This leads, for instance, to the CCR [22]

$$C_{\text{re}}(\rho_S) + P_{\text{vn}}(\rho_S) + S(\rho_S) = \log_2 d_S, \quad (1)$$

where $C_{\text{re}}(\rho_S)$ is the path relative entropy of coherence, $P_{\text{vn}}(\rho_S)$ is the von Neumann predictability, and $S(\rho_S)$ is the von Neumann entropy associated with a system S in the state ρ_S . Specifically, $C_{\text{re}}(\rho_S) := S(\rho_S || \Phi_Z(\rho_S))$, where $\Phi_Z(\rho_S) := \sum_{\eta} Z_{\eta} \rho_S Z_{\eta}$ denotes the output state of a non-selective measurement of $Z = \sum_{\eta} z_{\eta} Z_{\eta}$ with

projectors $Z_{\eta} = |\eta\rangle\langle\eta|$ associated with paths of the interferometer. Also, $P_{\text{vn}}(\rho_S) := S(\Phi_Z(\rho_S) || \Phi_{ZX}(\rho_S)) = S^{\max} - S(\Phi_Z(\rho_S))$, where X is a discrete-spectrum observable whose eigenbasis is mutually unbiased to the eigenbasis of Z . It measures how much the probability distribution associated with $\Phi_Z(\rho_S)$ differs from the uniform probability distribution I_S/d_S . Finally, $S(\rho_S)$ can be thought of as the relative entropy of entanglement between system S and the purification system.

This work follows recent efforts to investigate the interplay between gravity and quantum mechanics and to testify general relativistic effects in quantum phenomena [32–47]. To conduct our analysis, we consider a massive system with an internal spin. A boost to this system also affects the spin through Wigner rotations [48–50]. Our objective is to study how these relativistic effects (associated with time dilation) affect the interplay between the quantities in complementarity relations and, specifically, the CCR in Eq. (1) in a general spacetime. The reason this CCR was chosen is that, despite the long discussion about entanglement in relativistic scenarios [32, 51–56], Eq. (1) has been shown to be Lorentz invariant [57–59].

We focus our analysis on the dynamics of the system while it travels delayed-choice interferometers. This is motivated by the fact that these interferometers are typically built with the purpose of testing the complementarity principle. The original version of this type of experiment, proposed by Wheeler [60, 61], consists of a standard Mach-Zehnder interferometer with a phase shifter in one of the paths and one important modification: the experimentalist can either add or not the second beam splitter (BS) at will. If they choose to add it, statistics associated with a wave-like behavior are obtained, while particle-like statistics are observed if the second BS is not included in the interferometer. Crucially, the experimentalist can make their choice after the system enters the

* marcoslwbasso@hotmail.com

† ismaellpaiva@gmail.com

‡ dieguez.pr@gmail.com

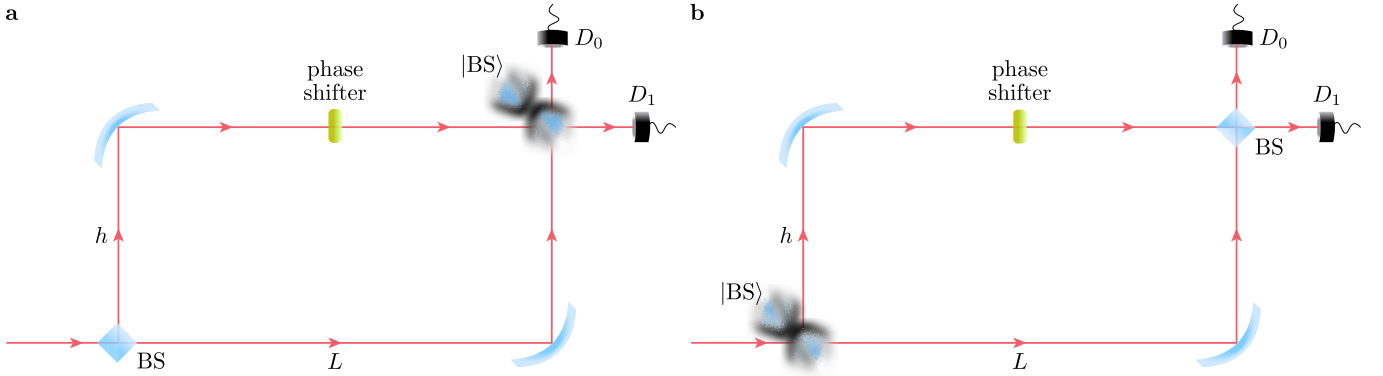


FIG. 1. **Schematic representation of the delayed-choice experiments.** **a** In the quantum delayed-choice experiment (QDCE), proposed in Ref. [31], the system enters an interferometer with an unbiased beam splitter (BS) and a phase shifter that implements a relative phase between the two paths. A second BS is considered in a coherent spatial superposition of being *in* and *out* of the interferometer. **b** In the quantum-controlled reality experiment (QCREE), introduced in Ref. [28], the experimental arrangement is based on switching the BSs in the QDCE. The first BS is now taken to be in a quantum coherent superposition of being *in* and *out* of the interferometer. It is noteworthy that, besides this difference, both experimental arrangements lead to the same interferometric visibility.

interferometer.

However, we consider generalizations of this original version that moved beyond the delayed-choice aspect of it. Precisely, we are interested in two variations, known as quantum delayed-choice experiment (QDCE) [31] and quantum-controlled reality experiment (QCREE) [28]. QDCE consists of a Mach-Zehnder in which the BS at the end of the interferometer is prepared in a quantum superposition of being present and absent in the interferometer path, as represented in Fig. 1a. Observe that the BS at the beginning of the interferometer is standard. This interferometer attracted attention because its output presents statistics that apparently are a hybrid of wave and particle [62–66], but its precise consequence to the understanding of the complementarity principle is still up for debate (see, e.g., Refs. [16, 67, 68]).

QCREE, on the other hand, modifies the QDCE to ensure that systems traveling inside the interferometer have a hybrid wave-and-particle behavior from the perspective of an entropic measure dubbed realism [69]. To achieve this, the standard BS and the one prepared in a superposition were switched, as illustrated in Fig. 1b. While this interferometer has the same visibility as the QDCE, it establishes a monotonic relation between the output visibility with the wave and particle realism [28].

In what follows, we study the CCR for the QDCE and QCREE in a non-relativistic scenario. This serves as a basis for comparison with our next results, which deal with these interferometers embedded in a general space-time. Once this is done, we make our discussion more concrete with an investigation of the Newtonian limit of our results. Meanwhile, in Appendixes A, B, D, and E, we briefly present the relevant background to this work and technical derivations. Also, in Appendix C, we introduce a conceptual discussion that shows a potential issue brought by Wigner rotations to operational approaches for time as an internal degree of freedom in quantum the-

ory. Finally, in Appendix F, we examine how relativist effects may alter the discussions about delayed choices in the configurations of interest in this work.

II. RESULTS

A. Non-relativistic treatment

Before studying the relativistic treatment of QDCE and QCREE, we first present a non-relativistic analysis of these experiments, since they had not been investigated with the CCR in Eq. (1) in the literature yet.

We start with the so-called quantum version of Wheeler's delayed-choice experiment (QDCE) proposed in Ref. [31] and depicted in Fig. 1a. Denoting $\{0, 1\}$ as the paths to be traveled in the interferometer and $|\psi_i\rangle = |0\rangle \otimes |\text{BS}\rangle$ as the initial state, with $|\text{BS}\rangle \equiv \cos \alpha |in\rangle + \sin \alpha |out\rangle$ representing a beam splitter (BS) in a coherent superposition of being present (in) and absent (out) of the interferometer with $0 \leq \alpha \leq \pi/2$. The joint system can be described right after the phase shifter introduced in path 1 as

$$|\psi_{\text{QDCE}}\rangle = \frac{1}{\sqrt{2}} (|0\rangle + e^{i\phi} |1\rangle) |\text{BS}\rangle. \quad (2)$$

At this stage, this is a separable state that does not yet contain any correlation between the particle and the BS in superposition. In fact, the state is unchanged until right before the system passes through the BS.

With this, we can readily construct the CCR in Eq. (1) for a system in this region of the interferometer. Indeed, it is straightforward that predictability and entanglement vanish for the state in Eq. (2), while coherence between the paths is maximum. Hence, there is no trade-off between the different quantities of the CCR, a similar char-

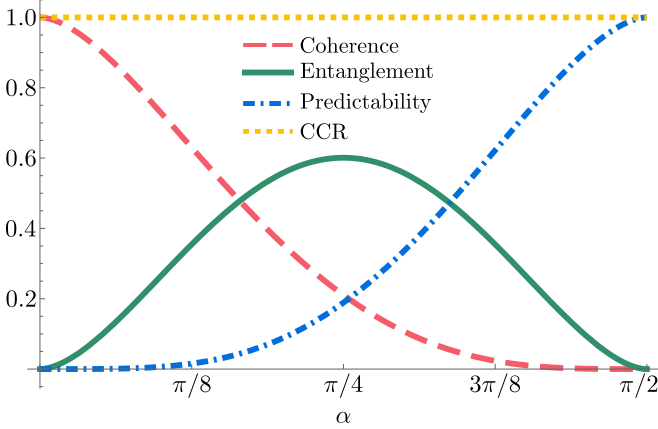


FIG. 2. **CCR for the non-relativistic QCRE as a function of α .** The plot shows how coherence and predictability follow a monotonic relation with the angle α , while the entanglement is maximum when the quantum controller has maximal initial coherence.

acteristic observed in Ref. [28] from the realism perspective.

We can also compute the visibility associated with this configuration. Indeed, observe that the output state right after the BS in superposition is

$$|\psi_f\rangle = \frac{1}{\sqrt{2}} \cos \alpha (|x+\rangle + e^{i\phi} |x-\rangle) |in\rangle + \frac{1}{\sqrt{2}} \sin \alpha (|0\rangle + e^{i\phi} |1\rangle) |out\rangle, \quad (3)$$

where $|x\pm\rangle = (|0\rangle \pm |1\rangle)/\sqrt{2}$ is written in the standard Pauli notation. The probability distribution for the detector D_0 at the output of the interferometer reads

$$p_0 = \frac{1}{2} (1 + \mathcal{V} \cos \phi), \quad (4)$$

where

$$\mathcal{V} := \frac{p_0^{\max} - p_0^{\min}}{p_0^{\max} + p_0^{\min}} = \cos^2 \alpha \quad (5)$$

is the final interferometric visibility.

Now, let us consider the quantum-controlled reality experiment (QCRE) proposed in Ref. [28], which is schematically represented in Fig. 1b. Again, we assume the initial state of the joint system to be the same $|\psi_i\rangle$ as before. However, $|\text{BS}\rangle$ refers to the state of the first BS this time around. Then, after the BS in superposition and the phase shifter on path 1, the joint system can be described as

$$|\phi_{\text{QCRE}}\rangle = \frac{1}{\sqrt{2}} \cos \alpha (|0\rangle + e^{i\phi} |1\rangle) |in\rangle + \sin \alpha |0\rangle |out\rangle. \quad (6)$$

Again, this state is kept unmodified until right before the second (standard) BS.

We can then compute the CCR associated with $|\phi_{\text{QCRE}}\rangle$. First, we trace out the BS to obtain the reduced density matrix of the system traveling the interferometer $\rho_S = \text{Tr}_{\text{BS}} |\phi_{\text{QCRE}}\rangle \langle \phi_{\text{QCRE}}|$, which gives

$$\rho_S = \frac{1}{2} \begin{pmatrix} 2 - \cos^2 \alpha & e^{-i\phi} \cos^2 \alpha \\ e^{i\phi} \cos^2 \alpha & \cos^2 \alpha \end{pmatrix}. \quad (7)$$

Hence, the path coherence is

$$C_{\text{re}}(\rho_S) = h\left(\frac{\cos^2 \alpha}{2}\right) - h\left(\frac{1+\lambda_\alpha}{2}\right), \quad (8)$$

where $h(u) := -u \log_2 u - (1-u) \log_2 (1-u)$ is the binary entropy and

$$\lambda_\alpha := \sqrt{2 \cos^4 \alpha - 2 \cos^2 \alpha + 1}. \quad (9)$$

The predictability is

$$P_{\text{vn}}(\rho_S) = 1 - h\left(\frac{\cos^2 \alpha}{2}\right). \quad (10)$$

Finally, the reduced entropy, in this case, amounts to the entanglement between the system and the BS. Its value is

$$S(\rho_S) = h\left(\frac{1+\lambda_\alpha}{2}\right). \quad (11)$$

Therefore, differently from the QDCE, we see a complementary trade-off between the components of the CCR, as shown in Fig. 2. However, as we discuss next, this observation about the QDCE is modified when considering general relativistic effects. Indeed, as will be seen, a trade-off relation exists in both QDCE and QDCE in this case.

Before concluding, we can also obtain the visibility associated with this setup. Observe that the output state reads

$$|\phi_f\rangle = \frac{1}{\sqrt{2}} \cos \alpha (|x+\rangle + e^{i\phi} |x-\rangle) |in\rangle + \sin \alpha |x+\rangle |out\rangle. \quad (12)$$

With this, it can be shown that this state is associated with precisely the same probability distribution in the ports D_0 and D_1 as the QDCE [28]. Consequently, both QDCE and QCRE have the same visibility.

B. Relativistic treatment

Now, we present our main results and discuss the CCR in the QDCE and QCRE in curved spacetime with a spin-1/2 particle. While we focus on these configurations, the general results that we present now are valid regardless of the shape of the interferometers. The geometry of the interferometer will play a more important role in Section II C, when we make our analysis more concrete by considering systems in the vicinity of Earth.

The study of spin-1/2 particles in a generic spacetime requires the use of local reference frames (LRFs) [32, 70],

which are briefly reviewed in Appendix A. In this scenario, it turns out that translations in spacetime have an interesting property: besides affecting the description of the particle's momentum, as in a standard relativistic boost, it also introduces a rotation to the system's spin [48–50], known as Wigner rotation. An introduction to the subject is presented in Appendix B.

This rotation is a function of the spacetime and the momentum of the wave function. In the case of our analysis, we will consider wave packets traveling the paths $|0\rangle$ and $|1\rangle$ in a coherent superposition. As discussed in Appendix D, each of these packets is assumed to be effectively associated with (possibly distinct) momenta \bar{p}_0 and \bar{p}_1 . Each path η is generally associated with distinct Wigner rotations $D(W(x_\eta, \tau_\eta))$, where x_η is the location of the center of mass of the wave packet on path η and τ_η is its proper time.

To start our analysis, consider the QDCE setup depicted in Fig. 1a in a relativistic scenario, including the presence of curved spacetime. As usual, we assume the system starts in the state

$$|\Psi_i\rangle = |0\rangle \otimes |\tau\rangle \otimes |\text{BS}\rangle, \quad (13)$$

where $|\tau\rangle$ refers to the initial state of the particle's spin and $|\text{BS}\rangle \equiv (|\text{in}\rangle + |\text{out}\rangle)/\sqrt{2}$ refers to the second BS, which is in a superposition of being present ($|\text{in}\rangle$) or absent ($|\text{out}\rangle$) of the interferometer path.

Following this, the phase shifter is applied to the system. Then, right after this and before the second BS, the state of the joint system is

$$|\Psi_{\text{QDCE}}\rangle = \frac{1}{\sqrt{2}} (|0\rangle |\tau_0\rangle + e^{i\phi} |1\rangle |\tau_1\rangle) \otimes |\text{BS}\rangle, \quad (14)$$

where $|\tau_\eta\rangle \coloneqq D(W(x_\eta, \tau_\eta))|\tau\rangle$, with $\eta \in \{0, 1\}$. Observe that the state in Eq. (14) is not constant in this region of the interferometer. Indeed, the states $|\tau_0\rangle$ and $|\tau_1\rangle$ are generally rotated along the path.

From Eq. (14), one can see that we have a separable state between the degrees of freedom of the particle and the BS in superposition. However, the spacetime geometry entangles the paths with the spin states. As a result, the reduced density matrix of the paths in superposition, $\rho_S = \text{Tr}_{\text{spin,BS}} |\Psi_{\text{QDCE}}\rangle \langle \Psi_{\text{QDCE}}|$, is given by

$$\rho_S = \frac{1}{2} \begin{pmatrix} 1 & e^{-i\phi} \langle \tau_1 | \tau_0 \rangle \\ e^{i\phi} \langle \tau_0 | \tau_1 \rangle & 1 \end{pmatrix}. \quad (15)$$

From this, we see that the CCR should be affected by time dilation since the coherence of ρ_S is affected by the entanglement between the paths and the spin.

To be more precise, we can then compute the elements of the CCR of a system in this region of the interferometer. By direct calculation, it follows that $S(\rho_S) = h(w)$, where $w = \frac{1}{2}(1 + |\langle \tau_0 | \tau_1 \rangle|)$, and $S(\Phi_Z(\rho_S)) = 1$. These, in turn, imply that the coherence associated with the paths is

$$C_{\text{re}}(\rho_S) = 1 - h \left(\frac{1}{2}(1 + |\langle \tau_0 | \tau_1 \rangle|) \right), \quad (16)$$

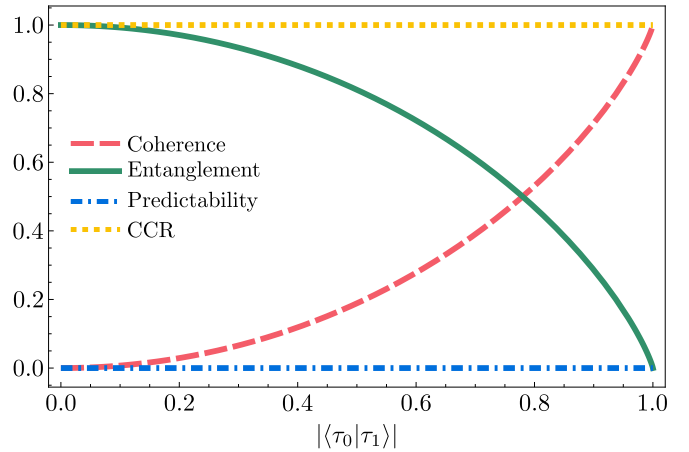


FIG. 3. **CCR for a particle undergoing the QDCE as a function of the relative Wigner rotations $|\langle \tau_0 | \tau_1 \rangle|$.** The graph shows how relativistic effects generally create a trade-off between coherence and entanglement. This differs from the standard (non-relativistic) scenario, which is equivalent to the case $|\langle \tau_0 | \tau_1 \rangle| = 1$, where entanglement vanishes. The predictability is not affected by the rotations.

while the predictability is

$$P_{\text{vn}}(\rho_S) = 0 \quad (17)$$

and the reduced entropy, which in this case can be associated with the amount of entanglement between the paths and the spin, is

$$S(\rho_S) = h \left(\frac{1}{2}(1 + |\langle \tau_0 | \tau_1 \rangle|) \right). \quad (18)$$

In Fig. 3, we can see how these quantities change as a function of the relative Wigner rotation between the arms in this setup. Since predictability vanishes, coherence and entanglement are free to oscillate in their full range, in a complementary manner. Depending on the spacetime curvature and the dimensions of the interferometer, multiple periods of these oscillations may take place while the particle traverses the interferometer. As will be seen, this does not happen to be the case in the Newtonian limit for reasonable interferometric's sizes. In any case, as discussed in Appendix F, the changes associated with Wigner rotations may generally have implications for discussions about the effects of “delayed choices” in these experiments.

Finally, we can analyze the visibility of the relativistic QDCE. Right after the second BS (which is in a superposition), the state of the joint system is

$$|\Psi_f\rangle = \frac{1}{\sqrt{2}} \cos \alpha (|x+\rangle |\tau_0\rangle + e^{i\phi} |x-\rangle |\tau_1\rangle) |\text{in}\rangle + \frac{1}{\sqrt{2}} \sin \alpha (|0\rangle |\tau_0\rangle + e^{i\phi} |1\rangle |\tau_1\rangle) |\text{out}\rangle. \quad (19)$$

Therefore, the probability of detection in D_η , $\eta \in \{0, 1\}$,

is given by

$$p_\eta = \frac{1}{2} [1 + (-1)^\eta |\langle \tau_0 | \tau_1 \rangle| \cos \phi \cos^2 \alpha], \quad (20)$$

which implies that the visibility is

$$\mathcal{V} = |\langle \tau_0 | \tau_1 \rangle| \cos^2 \alpha = \left| \cos \left(\frac{\Theta(1) - \Theta(0)}{2} \right) \right| \cos^2 \alpha, \quad (21)$$

where $\Theta(\eta)$ denotes the net Wigner rotation along path η , which can be completely characterized by the spacetime metric, the path η , and the initial state of the particle's spin. Observe that now we have a combination of the cosine due to the quantum-controlled beam splitter and the cosine due to the relative Wigner rotation along the paths.

Now, let us consider the QCRC in a relativistic scenario. The initial state $|\Phi_i\rangle$ of the system is again given by Eq. (13) but this time $|\text{BS}\rangle$ refers to the first BS.

Then, after the interaction with the BS in superposition and passing through the phase shifter, the joint system evolves to

$$|\Phi_{\text{QCRC}}\rangle = \frac{1}{\sqrt{2}} \cos \alpha (|0\rangle |\tau_0\rangle + e^{i\phi} |1\rangle |\tau_1\rangle) |\text{in}\rangle + \sin \alpha |0\rangle |\tau_0\rangle |\text{out}\rangle. \quad (22)$$

Here, again, the wave packet traveling on each path is effectively associated with a momentum \bar{p}_η , where η indicates the path. The momentum of distinct paths may have distinct values. Also, like in the QDCE, observe that the states $|\tau_0\rangle$ and $|\tau_1\rangle$ are generally rotated along the path. Thus the above state is not constant in this region of the interferometer. In any case, this expression shows that coherence between the paths is generally affected by time dilation. Indeed, the reduced density matrix of the main system $\rho_S = \text{Tr}_{\text{spin,BS}} |\Phi_{\text{QCRC}}\rangle \langle \Phi_{\text{QCRC}}|$ is

$$\rho_S = \frac{1}{2} \begin{pmatrix} 2 - \cos^2 \alpha & e^{-i\phi} \cos^2 \alpha \langle \tau_1 | \tau_0 \rangle \\ e^{i\phi} \cos^2 \alpha \langle \tau_0 | \tau_1 \rangle & \cos^2 \alpha \end{pmatrix}. \quad (23)$$

Now, we calculate the components of the CCR of a system in this region of the relativistic QCRC. Observe that the path coherence can be written as

$$C_{\text{re}}(\rho_S) = h\left(\frac{2 - \cos^2 \alpha}{2}\right) - h\left(\frac{1 + \lambda_{\alpha'}}{2}\right), \quad (24)$$

where

$$\lambda_{\alpha'} := \sqrt{|\langle \tau_0 | \tau_1 \rangle|^2 \cos^2 \alpha + (1 - \cos^2 \alpha)^2}. \quad (25)$$

Moreover, the predictability is

$$P_{\text{vn}}(\rho_S) = 1 - h\left(\frac{2 - \cos^2 \alpha}{2}\right). \quad (26)$$

Finally, the reduced entropy, in this case, can be understood as the amount of entanglement between the paths and the bipartition given by the spin+BS. Its value is

$$S(\rho_S) = h\left(\frac{1 + \lambda_{\alpha'}}{2}\right). \quad (27)$$

In Fig. 4, we can see the trade-off between these quantities in this setup. Similarly to the QDCE, predictability is insensitive to Wigner rotations. However, it does not vanish in general. Indeed, its value grows with α . This imposes a constraint on the interplay between coherence and entanglement, which can no longer oscillate in their full range. For coherence, this means that it decreases its amplitude, becoming closer to a vanishing constant while α grows. The entanglement, however, decreases its oscillation range approaching constant values that depend on α . This constant value also vanishes with α as the predictability value rises to 1. As is the case in the QDCE, the spacetime curvature and the dimensions of the interferometer may allow for little change or for multiple periods of these oscillations before the particle leaves the interferometer. Independently of this, we see that the maximum effect (in magnitude) of Wigner rotations in the CCR takes place when $\alpha = 0$.

To conclude, we can discuss the visibility associated with this setup. The state of the joint system after the second (standard) BS is

$$|\Phi_f\rangle = \frac{1}{\sqrt{2}} \cos \alpha (|x+\rangle |\tau_0\rangle + e^{i\phi} |x-\rangle |\tau_1\rangle) |\text{in}\rangle + \sin \alpha |x+\rangle |\tau_0\rangle |\text{out}\rangle. \quad (28)$$

Then, just like in the QDCE, the probability p_η is given by Eq. (20) for $\eta \in \{0, 1\}$ and, moreover, the visibility of the QCRC amounts to the quantity in Eq. (21).

C. Newtonian limit

To make the results just discussed more concrete, we now consider their Newtonian limit. This limit corresponds to the case of a weak and static gravitational field, such as in the vicinity of Earth, where the gravitational field can be considered uniform. The spacetime metric in this scenario can be expressed as

$$ds^2 = -(1 + 2gx)dt^2 + dx^2 + dy^2 + dz^2, \quad (29)$$

where $g = GM/R^2$ is Earth's gravitational acceleration in the origin of the laboratory frame ($x = 0$), which is at a distance R from the Earth's center. Moreover, the coordinate x measures the different heights (vertical axis) with respect to the origin of the laboratory frame. Moreover, we associate z with the horizontal axis coordinate. Observe that x is used here with a different meaning than it had in previous parts of this article.

We can then define a tetrad field that represents a static LRF by taking, at each point, the axes 0, 1, 2, and 3 to be parallel to the directions t , x , y , and z , respectively. Then, $e_t^0 = (1 + 2gx)^{1/2}$ and $e_x^1 = e_y^2 = e_z^3 = 1$, while every other component vanishes. The velocity components u^μ of the particle are taken such that the spatial components are constants. In addition, we assume that the speed u of both wave packets is the same and it is constant throughout the entire experiment. Hence, in the

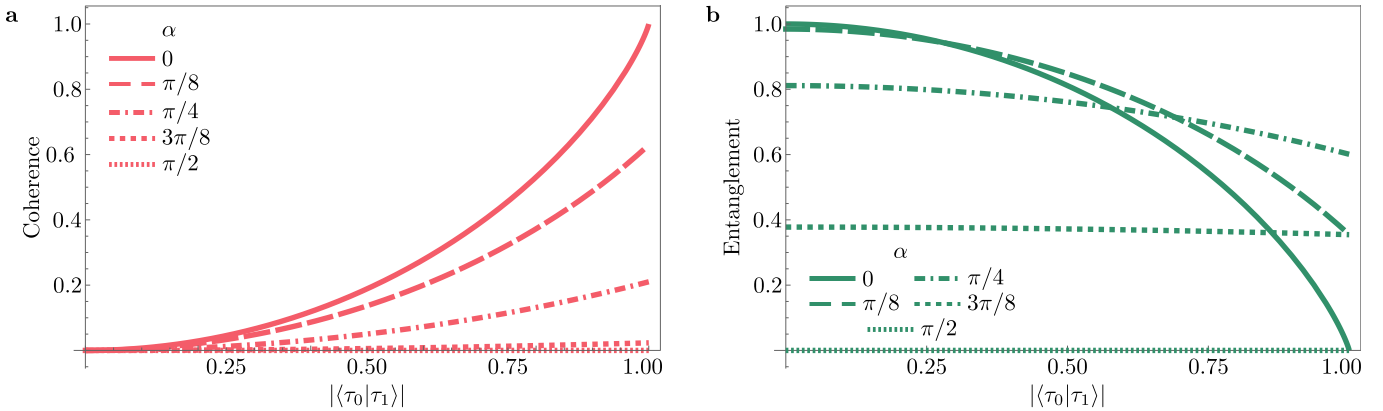


FIG. 4. Coherence and entanglement associated with the particle inside the QCRC as a function of the relative state of the particle's spin. When entering the interferometer, $|\langle \tau_0 | \tau_1 \rangle| = 1$. However, this value is generally modified while the particle traverses paths of the interferometer in superposition, introducing a dynamical trade-off between coherence and entanglement. While predictability is not affected by Wigner rotations, it depends on the parameter α , imposing constraints on the range of values coherence and entanglement may have. **a** It can be observed that, with an increase in α , the amplitude of values coherence can take decreases. Indeed, this quantity becomes close to a null constant. **b** The same decrease in the amplitude of values is seen for entanglement. However, it becomes close to a constant that depends on α , and is associated with the complement of predictability.

LRF, we have $u^0 = -u_0 = \sqrt{1+u^2}$, $u^1 = u_1 = u_x$, and $u^3 = u_3 = u_z$, where $u^2 = u_x^2 + u_z^2$. Observe that $u^y = 0$ since the particle's dynamics is restricted to the xz plane. Moreover, each wave packet is assumed to never move in a combination of the x and z directions simultaneously since we consider the interferometers with height h and horizontal length L in Fig. 1. Also, as discussed in Appendix C, to maximize the relativistic effects, we assume that $|\tau\rangle$ is any vector that belongs to the intersection between the Bloch sphere and the xz plane.

With this set, it follows that

$$|\langle \tau_0 | \tau_1 \rangle| = \left| \cos \left(\frac{(\Theta(1) - \Theta(0))}{2} \right) \right|, \quad (30)$$

where $\Theta(\eta)$ denotes the total Wigner rotation along the path $\eta \in \{0, 1\}$ up to the instant location of each wave packet in the laboratory frame, which is given by

$$\Theta(\eta) = -\gamma \frac{\ell_\eta(t)/u}{\sqrt{1+2g(x_0 + \eta h)}}, \quad (31)$$

where $\gamma = gu\sqrt{1+u^2}$, x_0 is the location of the lower horizontal path in the x axis, and $\ell_\eta(t)$ represents the horizontal length traveled by the wave packet until the instant t in the laboratory's clock. Details can be seen in Appendix E.

We are then ready to compute the elements of the CCR for both the QDCE and QCRC. From Eq. (31), we obtain

$$\Theta(1) - \Theta(0) = \gamma \left(\frac{\ell_0(t)/u}{\sqrt{1+2gx_0}} - \frac{\ell_1(t)/u}{\sqrt{1+2g(x_0 + h)}} \right) \quad (32)$$

This expression can be used in Eq. (30) to compute the distinguishability of the effects of Wigner rotations on

each path. In Fig. 5, the complement of $|\langle \tau_0 | \tau_1 \rangle|$ is shown as a function of time while a particle traverses squared interferometers with different sizes. We see that, for “reasonable lengths,” the distinguishability associated with the action of Wigner rotations on each path is extremely small. This means that these effects cannot be easily measured. In particular, as will be further discussed soon, the visibility, which is related to the values at the moment the particle leaves the interferometer, does not decrease much due to these gravitational effects. However, we observe that, relative to the final values, the spin states associated with the distinct paths are more differentiable in locations inside the interferometer.

We can also show that, in the Newtonian limit, the lengths considered in Fig. 5 can be largely increased while keeping the effects of Wigner rotations small. For this end, observe that the maximum change generated by Wigner rotations takes place at an instant t' such that $\ell_0(t') = L$ and $\ell_1(t') = 0$. In this case, Eq. (30) becomes $|\langle \tau_0 | \tau_1 \rangle| = |\cos(\gamma L/u)|$, where we have assumed that $x_0 = 0$. Using the second order approximation $\cos(x) \approx 1 - x^2/2$, it holds that

$$1 - |\langle \tau_0 | \tau_1 \rangle| = g^2(1+u^2)L^2. \quad (33)$$

In the international system of units, $u \rightarrow u/c$ and $gL \rightarrow gL/c^2$. Then, even if L were of the order of Earth's diameter, i.e., 10^8 m, the quantity in Eq. (33) would be of order 10^{-14} .

With Eq. (30), we have the needed ingredient to calculate the relevant quantities in the CCR for the QDCE in Eqs. (16), (17), and (18). Similarly, Eqs. (24), (26), and (27) can be computed, giving the CCR for the QCRC.

Before concluding, we can also discuss the visibility in the Newtonian limit. Since we are interested in the

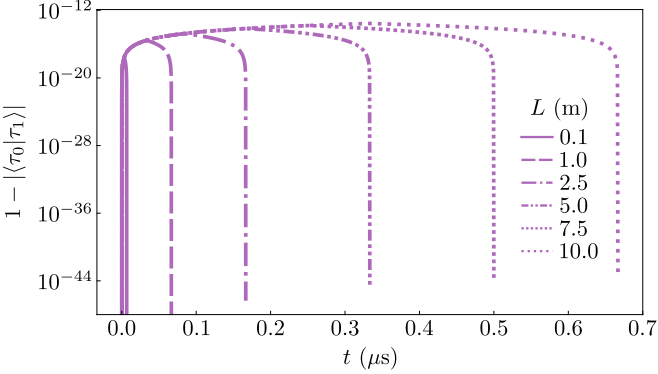


FIG. 5. **Distinguishability of relative Wigner rotations in the Newtonian limit while a particle encircles squared interferometers.** While this quantity, computed from Eqs. (30) and (32), is small at every location within the interferometer, its value at the instant the particle passes through the second BS is much lower than its maximum value inside. This implies a bigger influence of Wigner rotations in the CCR quantities than may be suggested by the interferometric visibility. It was assumed a particle's speed $u = 10^{-1}c$, $c = 3 \times 10^8$ m/s, $g = 10$ m/s², and $x_0 = 0$.

state of the system that leaves the interferometer, we have $\ell_\eta(t) = L$ for both paths η . Then,

$$\Theta(1) - \Theta(0) = \gamma \left(\frac{1}{\sqrt{1+2gx_0}} - \frac{1}{\sqrt{1+2g(x_0+h)}} \right) \Delta T, \quad (34)$$

where $\Delta T = L/u$ represents the time interval measured in the laboratory for each packet to travel in the horizontal direction. Using the approximation $(1+x)^{-1/2} \approx 1 - x/2$, we write

$$|\langle \tau_0 | \tau_1 \rangle| = \left| \cos \left(\frac{\gamma \Delta V \Delta T}{2} \right) \right|, \quad (35)$$

where $\Delta V = gh$ is the difference in the gravitational potential between the paths. This result can be replaced in Eq. (21) in order to compute the visibility of the QDCE and QCCE.

It is noteworthy that Eq. (35) is the same expression obtained for the visibility of the Mach-Zehnder interferometer in a relativistic treatment with the use of local Wigner rotations in the Newtonian limit [45]. Then, the visibility of the QDCE and QCCE can be seen as the associated visibility of the Mach-Zehnder interferometer modulated by a function of α .

In Fig. 6, we display the dependency of the visibility in the Newtonian limit (with the approximation used in Eq. (35)) as a function of α and ΔT . Observe that both the BS controller and the particle's spin can store at least partial which-way information. As a result, they both contribute to a decrease in the final interferometric visibility. Observe that, in the graphic, ΔT covers the entire domain needed for the quantity in Eq. (35) to change from 1 to 0. However, in current devices with appropriate scaling such that $\gamma \Delta V/2 = 1$ s⁻¹, ΔT takes values

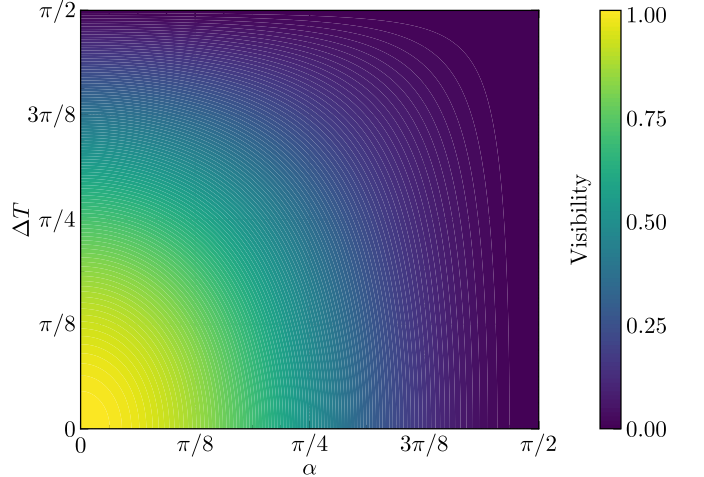


FIG. 6. **Visibility \mathcal{V} as a function of α and ΔT .** The visibility in Eq. (21) is calculated in the Newtonian limit with $|\langle \tau_0 | \tau_1 \rangle|$ given by Eq. (35). For simplicity, it was assumed that $\gamma \Delta V/2 = 1$ s⁻¹. Both the controller and the particle's spin store which-path information, contributing to the suppression of the interferometric visibility.

close to 0. This means that the reduction in visibility is minimum.

To give a more concrete notion of the order of magnitude of this effect, we can compare our expressions with the one obtained by Zych *et al.* [34], which derives similar consequences from the ones obtained here, albeit based on a different effect. In their approach, the authors relied on the internal degree of freedom of the system acting as a clock. The reported expression for $|\langle \tau_0 | \tau_1 \rangle|$ was $|\cos(\omega \Delta V \Delta T/2)|$, where ω is the frequency of the clock. From Eq. (35), we see that the difference in the expressions consists of the exchange $\omega \rightarrow \gamma$. If we use the international system of units, this becomes $\omega \rightarrow \gamma/c^2$. Then, even if we consider speeds of the order $u = 10^{-1}c$, we conclude that γ/c^2 is of order $1/c$. Meanwhile, as discussed in Ref. [34], the frequency of accurate clocks can be of order as high as 10^{15} Hz. As a consequence, the effect of Wigner rotations is much smaller than the effect associated with very precise internal clocks.

Two aspects of this conclusion deserve special attention. The first is that, despite the extra difficulty of measuring the results discussed here, they do not rely on the spin of the internal degree of freedom of the system to behave as a clock. This could be an advantage for the experimental verification in some platforms once enough resolution is reached. Moreover, they have a conceptual advantage from a theoretical perspective since they show that gravitational effects modify interferometric visibility even if the free Hamiltonian of the internal degree of freedom vanishes. In this sense, this generalizes the results of Ref. [34].

The other aspect is regarding the discussions in Appendix C. At least in a first analysis, Wigner rotations present a challenge to approaches that consider clocks

as internal degrees of freedom of quantum systems, as considered in Ref. [34]. However, as just seen, Wigner rotations do not affect the higher-order dynamics of the free Hamiltonian of the clock, at least in the vicinity of Earth. This means that the approach used in Ref. [34] is still valid to a large extent.

III. DISCUSSION

In this work, we have unveiled trade-offs between quantities in a CCR using generalized delayed-choice experiments (QDCE and QCRC) for that. We have presented a non-relativistic and relativistic analysis of these setups, including a more concrete study in the Newtonian limit. In the non-relativistic treatment, we have observed that, among the relevant quantities for the CCR, coherence is the only present inside the QDCE. Meanwhile, there is a trade-off between coherence, entanglement, and predictability inside the QCRC that depends directly on the parameter α that controls the superposition of the BS.

In the relativistic treatment, which involved an arbitrary (potentially curved) spacetime, it was assumed that the particle had an internal degree of freedom, chosen to be a spin for simplicity. Through Wigner rotations, the spin generally becomes correlated with the external degrees of freedom of the particle. This modifies the conclusions drawn in the non-relativistic scenario, and we have examined these changes in detail.

On the one hand, we have shown that there is now a trade-off between coherence and entanglement inside the QDCE. Predictability remains insensitive to Wigner rotations and vanishes. On the other hand, inside the QCRC, there also exists a similar trade-off between coherence and entanglement. The difference is that, while predictability is not affected by Wigner rotations, it is a function of α , like in the non-relativistic scenario. This adds a constraint in the range of values coherence and entanglement can take.

Moreover, we have proved that both interferometers have equal visibility. This holds in the non-relativistic and the relativistic treatments. In the relativistic case, the interferometric visibility generally decreases because it is modulated by a quantity associated with the overall effective Wigner rotation during the particle's travel. However, an increase in current measurement precision is needed for the observation of our predictions.

It is worth emphasizing that, while our results lead to smaller changes to predictions in the vicinity of Earth than previous works in the area, they do not rely on the particle traveling the interferometer having an internal clock. This means that the free Hamiltonian of the internal degree of freedom of the particle considered here may even vanish without invalidating our predictions. In this sense, our study generalizes the conclusion from Refs. [34, 35, 37, 39] that general relativity has a universal decoherence effect on quantum superpositions.

Finally, an interesting research avenue is the study of

multipath interferometry in relativistic scenarios. In this context, one could look for special configurations that enhance the effects of Wigner rotations, facilitating their practical observations.

ACKNOWLEDGMENTS

The authors would like to thank Eliahu Cohen and Augusto C. Lobo for their comments on a previous version of this manuscript, which greatly helped improve the presentation of our results. M.L.W.B. acknowledges financial support from the São Paulo Research Foundation (FAPESP), Grant No. 2022/09496-8. I.L.P. acknowledges financial support from the ERC Advanced Grant FLQuant. P.R.D. acknowledges support from the Foundation for Polish Science (IRAP project, ICTQT, Contract No. MAB/2018/5, co-financed by EU within Smart Growth Operational Programme).

Appendix A: Local reference frames and boosts

The central object of analysis in this work is particles with an internal structure, which, for simplicity, are taken to be a spin-1/2. Since their study in general spacetime requires the use of LRFs, we review them here.

LRFs are defined at each point x of a spacetime \mathcal{M} using a tetrad field (or vielbein), which is composed of 4-vectors $e_a^\mu(x)$, $a = 0, 1, 2, 3$, orthonormal to each other with respect to the pseudo-Riemannian manifold (or spacetime) [71], i.e., $e_\mu^a(x)e_b^\mu(x) = \delta_b^a$ and $e_\mu^a(x)e_a^\nu(x) = \delta_\mu^\nu$, where we have used the convention that Latin indices refer to coordinates in the LRF, Greek indices refer to the general coordinate system defined in the spacetime \mathcal{M} , and repeated indices are summed over. Thus, at each point $x \in \mathcal{M}$, the Minkowski metric in the LRF, $\eta_{ab} = \text{diag}(-1, 1, 1, 1)$, and the spacetime metric, $g_{\mu\nu}(x)$, are related with the tetrad field according to [72]

$$\begin{aligned} g_{\mu\nu}(x)e_a^\mu(x)e_b^\nu(x) &= \eta_{ab}, \\ \eta_{ab}e_\mu^a(x)e_\nu^b(x) &= g_{\mu\nu}(x). \end{aligned} \quad (\text{A1})$$

For the general coordinate system, the lowering and raising of indices are done with the metric $g_{\mu\nu}$ and its inverse $g^{\mu\nu}$, respectively, while the indices in the LRF are lowered by η_{ab} and raised by its inverse η^{ab} . Furthermore, the components of the tetrad field and its inverse transform a tensor in the general coordinate system into one in the local frame and vice versa. Therefore, from Eq. (A1), one can see that the tetrad field incorporates the spacetime curvature information hidden in the metric. In addition, the vielbein $\{e_a^\mu(x), a = 0, 1, 2, 3\}$ is a set of four 4-vector fields and transforms under local Lorentz transformations (LLTs) in the local system. Observe that, since $e_0^\mu(x)$ is a time-like vector field defined at each point of the spacetime and produces a global time coordinate, it makes the spacetime time orientable [71].

Moreover, the LRF is not unique since it continues to be a LRF under LLTs. Thus, a vielbein representation of a given metric is not defined in a unique manner, and different vielbein connected by LLTs are associated with the same metric tensor [70].

Now, we follow the particle's path from one point to another in the curved spacetime \mathcal{M} to construct a representation for LLTs. For this, consider a system with four-momentum $p^\mu(x) = mu^\mu(x)$ at a certain location x , where m is the mass of the particle and $u^\mu(x)$ is its four-velocity. Using units such that $c = 1$, the momentum satisfies $p^\mu(x)p_\mu(x) = -m^2$. In the LRF at the point x whose coordinates are $x^a = e_\mu^a(x)x^\mu$, the momentum of the particle can be written as $p^a(x) = e_\mu^a(x)p^\mu(x)$. After an infinitesimal interval of proper time $d\tau$ has passed, the particle is found at a new location $x'^\mu = x^\mu + u^\mu d\tau$ with momentum $p^a(x') = p^a(x) + \delta p^a(x)$. The variation in momentum can be decomposed into two parts:

$$\delta p^a(x) = e_\mu^a(x)\delta p^\mu(x) + \delta e_\mu^a(x)p^\mu(x), \quad (\text{A2})$$

where the change due to the geometry of spacetime is encoded in δe_μ^a , while the change $\delta p^\mu(x)$ is associated with external non-gravitational forces. The variation $\delta p^\mu(x)$ can be written as

$$\begin{aligned} \delta p^\mu(x) &= u^\nu(x)\nabla_\nu p^\mu(x)d\tau \\ &= -\frac{1}{m}[a^\mu(x)p_\nu(x) - p^\mu(x)a_\nu(x)]p^\nu(x)d\tau, \end{aligned} \quad (\text{A3})$$

where $a^\mu := u^\nu\nabla_\nu u^\mu$ is the particle's four-acceleration. Moreover, the variation due to the geometry of spacetime can be written as

$$\delta e_\mu^a(x) = u^\nu(x)\nabla_\nu e_\mu^a(x)d\tau = -u^\nu(x)\omega_{\nu b}^a(x)e_\mu^b(x)d\tau, \quad (\text{A4})$$

where $\omega_{\nu b}^a := e_\lambda^\nu\nabla_\nu e_\lambda^a = -e_\lambda^\lambda\nabla_\nu e_\lambda^a$ is the spin connection [73]. Substituting these expressions in Eq. (A2), one obtains $\delta p^a(x) = \lambda_b^a(x)p^b(x)d\tau$, where

$$\lambda_b^a(x) := u^a(x)a_b(x) - a^a(x)u_b(x) - u^\nu(x)\omega_{\nu b}^a(x). \quad (\text{A5})$$

The tensor $\lambda_b^a(x)$ is interpreted as the infinitesimal LLT since it holds that $p^a(x') = [\delta_b^a + \lambda_b^a(x)d\tau]p^b(x)$ [70].

Appendix B: Wigner rotations

With LRFs and LLTs defined, we follow Refs. [32, 70] and introduce local Silberstein-Thomas-Wigner rotations [48–50], which will be simply referred to as Wigner rotations, as they are more commonly known in the physics community.

The joint state of a particle in an eigenstate of momentum with an internal spin can be denoted by $|p^a(x), \sigma; x^a, e_\mu^a(x), g_{\mu\nu}(x)\rangle$ to evidence its dependency on the vielbein $e_\mu^a(x)$ and $g_{\mu\nu}(x)$ as described from the position $x^a = e_\mu^a(x)x^\mu$ of the LRF. In this expression, $|\sigma\rangle$ is associated with the particle's internal degree of

freedom, i.e., the particle's spin. However, for simplicity, we identify

$$|p^a(x), \sigma\rangle \equiv |p^a(x), \sigma; x^a, e_\mu^a(x), g_{\mu\nu}(x)\rangle. \quad (\text{B1})$$

Generally, the particle will be in a linear combination of different momentum eigenstates, i.e., [70]

$$|\Psi\rangle = \int d\mu(\mathbf{p})\psi(\mathbf{p})|\mathbf{p}(x), \sigma\rangle. \quad (\text{B2})$$

However, as it will become clear, in order to construct the Wigner rotations, it is convenient to take the state of the system to be the one in Eq. (B1) for a given $p^a(x)$. In this case, it is possible to show that the particle and its internal degree of freedom transform under a spinorial unitary representation of the LLT [32, 70], i.e.,

$$U(\Lambda(x))|p^a(x), \sigma\rangle = |\Lambda p^a(x)\rangle \otimes D(W(x))|\sigma\rangle, \quad (\text{B3})$$

where $W(x) := W(\Lambda(x), p(x))$ is a local Wigner rotation and $D(W(x))$ is a unitary representation of the local Wigner rotation. Therefore, the state $|p^a(x), \sigma\rangle$ at point x is now described as $U(\Lambda(x))|p^a(x), \sigma\rangle$ at point x' , and Eq. (B3) expresses how the spin rotates locally as the quantum particle moves along its world line.

For an infinitesimal LLT, the corresponding infinitesimal local Wigner rotation can be written as $W_b^a(x) = \delta_b^a + \vartheta_b^a d\tau$ [74], where

$$\vartheta_j^i(x) = \lambda_j^i(x) + \frac{\lambda_0^i(x)p_j(x) - \lambda_{j0}(x)p^i(x)}{p^0(x) + m}, \quad (\text{B4})$$

with all other terms vanishing. Therefore, the spin-1/2 representation of the infinitesimal local Wigner rotation can be written as

$$\begin{aligned} D(W(x)) &= I_{2 \times 2} + \frac{i}{4} \sum_{i,j,k=1}^3 \epsilon_{ijk} \vartheta_{ij}(x) \sigma_k d\tau \\ &= I_{2 \times 2} + \frac{i}{2} \boldsymbol{\vartheta} \cdot \boldsymbol{\sigma} d\tau, \end{aligned} \quad (\text{B5})$$

where $I_{2 \times 2}$ is the identity matrix and σ_k , $k = 1, 2, 3$ are the well-known Pauli matrices. Finally, the spin-1/2 representation of the local Wigner rotation for a finite interval of proper time is obtained by iterating the expression above, which leads to [32]

$$D(W(x, \tau)) = \mathcal{T} e^{\frac{i}{2} \int_0^\tau \boldsymbol{\vartheta} \cdot \boldsymbol{\sigma} d\tau'}, \quad (\text{B6})$$

where \mathcal{T} is the time-ordering operator.

Appendix C: Spins and clocks

As previously explained, the spin rotates locally as the associate quantum particle moves along its world line according to the expression given by Eq. (B6). This rotation depends on the momentum of the particle and the

spacetime curvature. However, observe that the rotation magnitude is not always proportional to the proper time of a given wave packet. Hence, the spin does act as a clock as a result of these rotations. Nevertheless, it captures the existence of time dilation in some circumstances, as can be concretely seen in the Newtonian limit (Appendix E). This is why we use τ to denote the state of the particle's spin.

The reason the time-ordering operator \mathcal{T} is needed in Eq. (B6) is that, generally, the rotations at different points along the particle's trajectory do not commute with each other. This means that, indeed, the spin is generally affected by Wigner rotations regardless of its initial state. However, in some instances, rotations at distinct instants of proper time might commute, i.e., they might be about a single axis. In these cases, particular initial states would not be affected by it. For example, as is the case in Section II C, the Wigner rotation might be a rotation about the y axis. Then, eigenstates of σ_y would not be modified and become correlated to the external degree of freedom of the particle. Moreover, while any other initial state could register the rotation in this scenario, a spin's dynamics on the xz plane, i.e., the equator of the y axis, would be optimal, in the sense of allowing for the best distinguishability between states rotated in different manners. Therefore, in this work, we take the initial state of the spin to be any state in the aforementioned equator.

It turns out that this choice is consistent with the prescription to build time states in the Page and Wootters framework [75], which has also been studied in relativistic and/or gravitational scenarios [76–83]. This is a framework for relational dynamics in which time is not an *a priori* parameter. Instead, it is given by a set of states, dubbed time states, from a physical system used as a clock. To construct the set of time states, one first chooses a reference state $|t'\rangle$ in the clock system. The other time states are defined as $|t\rangle := e^{-iH_C(t-t')}|t'\rangle$, where H_C is the Hamiltonian of the clock. However, the set of states $|t\rangle$ should be such that $\int dt |t\rangle\langle t| = I_C$, where I_C is the identity operator, which shows that the reference state $|t'\rangle$ should be appropriately chosen. In general, the resulting time operator $T = \int dt t|t\rangle\langle t|$ is a positive operator-valued measure, but not necessarily a Hermitian operator [76, 84, 85]. In the case of a clock given by a spin with a Hamiltonian proportional to σ_y , we see that time states should live in the xz plane, which indeed corresponds to the optimal choice discussed above for the state of the spin in the study in Section II C.

A question that deserves further investigation is whether Wigner rotations should be considered operational features of time revealed by quantum theory or a challenge to the relativistic treatment of clocks as internal degrees of freedom since they introduce modifications to the clock's state in addition to the relativistic time dilation, albeit related to it. In Ref. [86], even though this question is approached from a different perspective, the authors seem to agree with the latter.

Appendix D: Approximation for localized wave packets

Our brief introduction to Wigner rotations reveals that they depend on the momentum of the particle. Then, consider a particle in a state other than a plane wave, i.e., a generic state as given by Eq. (B2) with $\psi(\mathbf{p}) \neq \delta(\mathbf{p} - \bar{\mathbf{p}})$ for a constant momentum $\bar{\mathbf{p}}$. In this case, even if the spatial distribution of the particle and its spin start in a separable state, they generally evolve into an entangled state while the particle translates in space.

These exact calculations, however, do not typically lead to simple analytic solutions. Then, it is common to assume a wave packet with a mean centroid $\bar{\mathbf{p}}$ around which the particle momentum is properly distributed, e.g., $\psi_\sigma(\mathbf{p}) \propto e^{-(\mathbf{p}-\bar{\mathbf{p}})^2/\xi^2}$ for some positive real constant ξ . As a result, in the semiclassical approach, the motion of the particle can be regarded by the motion of its center of mass with momentum $\bar{\mathbf{p}}$. These ideas can be formalized with a Wentzel-Kramers-Brillouin expansion of the exact solution [70]. Indeed, the analysis just described here corresponds to the zeroth order expansion of the solution in \hbar . The centroid $\bar{\mathbf{p}}$ need not be constant throughout the dynamics. Indeed, the result is valid as long as the shape of the wave function is kept approximately unchanged during the experiment [71, 87]. These ideas can be extended to the case of packets traveling in a coherent superposition of wave packets such that there is no distortion of the wave packet along the path, where each packet can be associated with different centroid values $\bar{\mathbf{p}}$. A more detailed discussion can be found in Refs. [46, 87, 88].

These remarks play an important role in Section II, where we consider a particle traveling an interferometer in a coherent superposition of paths. We assume that the motion of the wave packet traveling on each path can be characterized by its mean centroid momentum, as just discussed. Consequently, each path will be associated with a well-defined time dilation.

Appendix E: Derivations for the Newtonian limit

Given the construction of the tetrads and the conditions described in Section II C, we now derive the main results presented there. Since the interferometer paths are not geodesic, an external force is necessary to maintain the particle in such a world line. The non-vanishing components of the acceleration due to the external force are

$$a^0(x) = \frac{gu_x\sqrt{1+u^2}}{1+2gx}, \quad a^1(x) = \frac{g(1+u^2)}{1+2gx}. \quad (\text{E1})$$

To obtain the infinitesimal LLT, Eq. (A5) shows that we first need to compute the spin connection $\omega_{\nu b}^a$. Observe that

$$\omega_{\nu b}^a = -e_b^\lambda \partial_\nu e_\lambda^a + \Gamma_{\nu\lambda}^\sigma e_\sigma^a e_b^\lambda = \Gamma_{\nu\lambda}^\sigma e_\sigma^a e_b^\lambda, \quad (\text{E2})$$

where $\Gamma_{\nu\lambda}^\sigma$ is the Christoffel symbol. It can be verified that the only non-zero Christoffel symbols are given by $\Gamma_{tt}^x = g$ and $\Gamma_{tx}^t = \Gamma_{xt}^t = g/(1+2gx)$. Then, by symmetry, we conclude that the non-vanishing components of the spin connection are

$$\begin{aligned}\omega_{t1}^0 &= \frac{g}{\sqrt{1+2gx}}, \\ \omega_{x1}^0 &= g\sqrt{1+2gx}.\end{aligned}\quad (\text{E3})$$

As a result, the non-zero infinitesimal LLTs are given by

$$\begin{aligned}\lambda_1^0(x) &= \frac{g\sqrt{m^2+p^2}}{m^3(1+2gx)}(p^2-p_x^2) - \frac{\sqrt{1+2gx}}{m}p_x, \\ \lambda_3^0(x) &= -\frac{gp_xp_z\sqrt{m^2+p^2}}{m^3(1+2gx)}, \\ \lambda_3^1(x) &= -\frac{gp_z(m^2+p^2)}{m^3(1+2gx)},\end{aligned}\quad (\text{E4})$$

where $p = \sqrt{p_x^2 + p_z^2}$. Therefore, the only non-null element of the Wigner rotation in parts of the path is ϑ_3^1 . On the horizontal portions of the paths, $p_z = 0$ and hence Eq. (B4) implies that $\vartheta_3^1 = 0$. On the vertical portions of the paths, $p_x = 0$ and

$$\vartheta_3^1(x) = -\frac{gp_z\sqrt{p_z^2+m^2}}{(1+2gx)m^2}.\quad (\text{E5})$$

From the above expression, we see that the Wigner rotation, when non-null, depends on g and on the height x .

The relevant quantity we want to calculate is $|\langle\tau_0|\tau_1\rangle|$, which is the same for both QDCE and QCRC. As a matter of fact, given a spacetime metric, this quantity only depends on the spatial geometry of the interferometer. Using the quantities introduced here, we have

$$|\langle\tau_0|\tau_1\rangle| = \left| \langle\tau|e^{-\frac{i}{2}\sigma_y(\Theta(1)-\Theta(0)}}|\tau\rangle \right|,\quad (\text{E6})$$

where

$$\Theta(\eta) := \int_0^\tau d\tau' \vartheta_3^1(x(\tau';\eta))\quad (\text{E7})$$

for $\eta \in \{0,1\}$. This leads to Eq. (30) if $|\tau\rangle$ is a pure state in the intersection between the Bloch sphere and the xz plane, as it has been assumed. Clearly, only the horizontal regions of each path contribute to $\Theta(\eta)$.

Now, we would like to parametrize the paths in terms of the time t measured by the laboratory frame. Since $-d\tau^2 = g_{\mu\nu}dx^\mu dx^\nu$, we have

$$\frac{d\tau}{dt} = \sqrt{-g_{tt} - g_{ij}\frac{dx^i}{dt}\frac{dx^j}{dt}}.\quad (\text{E8})$$

The first term in the square root corresponds to the gravitational time dilation, while the second term corresponds to the special relativistic time dilation. However, if the

trajectories are such that the speed of both wave packets is the same and it is constant throughout the entire experiment, as we assume here, there will be no time dilation stemming from special relativity [34]. As a result, from Eq. (E8), we are only left with the first term in the square root. Then, since

$$\Theta(\eta) = \int_0^t dt' \frac{d\tau'}{dt'} \vartheta_3^1(x(t';\eta)),\quad (\text{E9})$$

we are led to Eq. (31).

Appendix F: The delayed-choice aspect

As already mentioned, the QDCE and QCRC are typically discussed in contexts in which the “delayed choice” aspect is less integral to the experiment, in the sense that classical particle-like and wave-like behaviors are said to be probed simultaneously. However, the standard delayed-choice notion can be represented by conditioning the outcome of the interferometer on a post-selection of the quantum-controlled BS in a state that corresponds to it being inside or outside the interferometer. This choice can even be postponed to the moment after the interferometric experiment has even been recorded, a scenario that is not possible in the original version of the experiment. Answering the question of whether a future action affects the past behavior of a quantum system will generally depend on the choice of interpretation of quantum mechanics. Nevertheless, some consequences can be drawn about this aspect that follows directly from the mathematical formalism we have used in our derivations, thus shedding new light on this fundamental debate.

On the one hand, in the QDCE, the state of the particle inside the interferometer is unmodified regardless of the post-selection made on the BS. It also does not depend on when such a post-selection is made. However, because of the entanglement with the particle’s spin, path coherence is not constant inside the interferometer and might be at a much smaller level relative to the non-relativistic case when the particle leaves. If this were the case, it would lead to statistics that could be more easily associated with a classical particle-like behavior since final interferometric visibility will be suppressed due to relativistic effects. This is independent of the choice of post-selection of the BS.

On the other hand, in the QCRC, it can be observed that the state assigned to the system inside the interferometer depends on the post-selection of the BS. If BS is post-selected outside the interferometer, both coherence and entanglement vanish, and predictability is maximum. Indeed, in this case, the system’s state corresponds to a single packet traveling on path 0. However, if the BS is post-selected inside the interferometer, then predictability vanishes, and we have the exact interplay seen inside the QDCE.

It is worth emphasizing that these modifications are minimum in the vicinity of Earth, as discussed in Section

II C. This is the case because Wigner rotations have small magnitudes in this scenario. Nevertheless, our results

indicate that this effect can be more relevant in other curved spacetime.

[1] N. Bohr, The quantum postulate and the recent development of atomic theory, *Nature* **121**, 580 (1928).

[2] N. Bohr, Can quantum-mechanical description of physical reality be considered complete?, *Phys. Rev.* **48**, 696 (1935).

[3] V. Jacques, E. Wu, F. Grosshans, F. Treussart, P. Grangier, A. Aspect, and J.-F. Roch, Experimental realization of Wheeler's delayed-choice gedanken experiment, *Science* **315**, 966 (2007).

[4] A. G. Manning, R. I. Khakimov, R. G. Dall, and A. G. Truscott, Wheeler's delayed-choice gedanken experiment with a single atom, *Nat. Phys.* **11**, 539 (2015).

[5] F. Vedovato, C. Agnesi, M. Schiavon, D. Dequal, L. Calderaro, M. Tomasin, D. G. Marangon, A. Stanco, V. Luceri, G. Bianco, *et al.*, Extending Wheeler's delayed-choice experiment to space, *Sci. Adv.* **3**, e1701180 (2017).

[6] L. Catani, M. Leifer, D. Schmid, and R. W. Spekkens, Why interference phenomena do not capture the essence of quantum theory, [arXiv:2111.13727](https://arxiv.org/abs/2111.13727) (2021).

[7] L. Catani, M. Leifer, G. Scala, D. Schmid, and R. W. Spekkens, What aspects of the phenomenology of interference witness nonclassicality?, [arXiv:2211.09850](https://arxiv.org/abs/2211.09850) (2022).

[8] W. K. Wootters and W. H. Zurek, Complementarity in the double-slit experiment: Quantum nonseparability and a quantitative statement of Bohr's principle, *Phys. Rev. D* **19**, 473 (1979).

[9] D. M. Greenberger and A. Yasin, Simultaneous wave and particle knowledge in a neutron interferometer, *Phys. Lett. A* **128**, 391 (1988).

[10] B.-G. Englert, Fringe visibility and which-way information: An inequality, *Phys. Rev. Lett.* **77**, 2154 (1996).

[11] S. Dürr, Quantitative wave-particle duality in multibeam interferometers, *Phys. Rev. A* **64**, 042113 (2001).

[12] S. Saunders, Complementarity and scientific rationality, *Found. Phys.* **35**, 417 (2005).

[13] B.-G. Englert, D. Kaszlikowski, L. C. Kwek, and W. H. Chee, Wave-particle duality in multi-path interferometers: General concepts and three-path interferometers, *Int. J. Quantum Inf.* **6**, 129 (2008).

[14] T. Baumgratz, M. Cramer, and M. B. Plenio, Quantifying coherence, *Phys. Rev. Lett.* **113**, 140401 (2014).

[15] M. N. Bera, T. Qureshi, M. A. Siddiqui, and A. K. Pati, Duality of quantum coherence and path distinguishability, *Phys. Rev. A* **92**, 012118 (2015).

[16] R. M. Angelo and A. D. Ribeiro, Wave-particle duality: An information-based approach, *Found. Phys.* **45**, 1407 (2015).

[17] P. J. Coles, Entropic framework for wave-particle duality in multipath interferometers, *Phys. Rev. A* **93**, 062111 (2016).

[18] E. Bagan, J. A. Bergou, S. S. Cottrell, and M. Hillery, Relations between coherence and path information, *Phys. Rev. Lett.* **116**, 160406 (2016).

[19] E. Bagan, J. Calsamiglia, J. A. Bergou, and M. Hillery, Duality games and operational duality relations, *Phys. Rev. Lett.* **120**, 050402 (2018).

[20] S. Mishra, A. Venugopalan, and T. Qureshi, Decoherence and visibility enhancement in multipath interference, *Phys. Rev. A* **100**, 042122 (2019).

[21] M. L. W. Basso, D. S. S. Chrysosthemos, and J. Maziero, Quantitative wave-particle duality relations from the density matrix properties, *Quantum Inf. Process.* **19**, 254 (2020).

[22] M. L. W. Basso and J. Maziero, Complete complementarity relations for multipartite pure states, *J. Phys. A* **53**, 465301 (2020).

[23] M. L. W. Basso and J. Maziero, An uncertainty view on complementarity and a complementarity view on uncertainty, *Quantum Inf. Process.* **20**, 201 (2021).

[24] T. Qureshi, Predictability, distinguishability, and entanglement, *Opt. Lett.* **46**, 492 (2021).

[25] M. L. W. Basso and J. Maziero, Entanglement monotones from complementarity relations, *J. Phys. A* **55**, 355304 (2022).

[26] X.-F. Qian, K. Konthasinghe, S. K. Manikandan, D. Specker, A. N. Vamivakas, and J. H. Eberly, Turning off quantum duality, *Phys. Rev. Res.* **2**, 012016 (2020).

[27] M. Jakob and J. A. Bergou, Quantitative complementarity relations in bipartite systems: Entanglement as a physical reality, *Opt. Commun.* **283**, 827 (2010).

[28] P. R. Dieguez, J. R. Guimarães, J. P. Peterson, R. M. Angelo, and R. M. Serra, Experimental assessment of physical realism in a quantum-controlled device, *Commun. Phys.* **5**, 82 (2022).

[29] D. S. S. Chrysosthemos, M. L. W. Basso, and J. Maziero, Quantum coherence versus interferometric visibility in a biased Mach-Zehnder interferometer, *Quantum Inf. Process.* **22**, 68 (2023).

[30] R. Wagner, A. Camillini, and E. F. Galvão, Coherence and contextuality in a Mach-Zehnder interferometer, [arXiv:2210.05624](https://arxiv.org/abs/2210.05624) (2022).

[31] R. Ionicioiu and D. R. Terno, Proposal for a quantum delayed-choice experiment, *Phys. Rev. Lett.* **107**, 230406 (2011).

[32] H. Terashima and M. Ueda, Einstein-Podolsky-Rosen correlation in a gravitational field, *Phys. Rev. A* **69**, 032113 (2004).

[33] I. Fuentes-Schuller and R. B. Mann, Alice falls into a black hole: Entanglement in noninertial frames, *Phys. Rev. Lett.* **95**, 120404 (2005).

[34] M. Zych, F. Costa, I. Pikovski, and Č. Brukner, Quantum interferometric visibility as a witness of general relativistic proper time, *Nat. Commun.* **2**, 505 (2011).

[35] M. Zych, F. Costa, I. Pikovski, T. C. Ralph, and Č. Brukner, General relativistic effects in quantum interference of photons, *Class. Quantum Grav.* **29**, 224010 (2012).

[36] E. Martin-Martinez and N. C. Menicucci, Entanglement in curved spacetimes and cosmology, *Class. Quantum Grav.* **31**, 214001 (2014).

[37] I. Pikovski, M. Zych, F. Costa, and Č. Brukner, Universal decoherence due to gravitational time dilation, *Nat.*

Phys. **11**, 668 (2015).

[38] Y. Margalit, Z. Zhou, S. Machluf, D. Rohrlich, Y. Japha, and R. Folman, A self-interfering clock as a “which path” witness, *Science* **349**, 1205 (2015).

[39] M. Zych, I. Pikovski, F. Costa, and Č. Brukner, General relativistic effects in quantum interference of “clocks”, *J. Phys.: Conf. Ser.* **723**, 012044 (2016).

[40] S. Bose, A. Mazumdar, G. W. Morley, H. Ulbricht, M. Toroš, M. Paternostro, A. A. Geraci, P. F. Barker, M. S. Kim, and G. Milburn, Spin entanglement witness for quantum gravity, *Phys. Rev. Lett.* **119**, 240401 (2017).

[41] C. Marletto and V. Vedral, Gravitationally induced entanglement between two massive particles is sufficient evidence of quantum effects in gravity, *Phys. Rev. Lett.* **119**, 240402 (2017).

[42] M. Christodoulou and C. Rovelli, On the possibility of laboratory evidence for quantum superposition of geometries, *Phys. Lett. B* **792**, 64 (2019).

[43] R. Howl, R. Penrose, and I. Fuentes, Exploring the unification of quantum theory and general relativity with a Bose-Einstein condensate, *New J. Phys.* **21**, 043047 (2019).

[44] A. Roura, Gravitational redshift in quantum-clock interferometry, *Phys. Rev. X* **10**, 021014 (2020).

[45] M. L. W. Basso and J. Maziero, Interferometric visibility in curved spacetimes, *Class. Quantum Grav.* **38**, 135007 (2021).

[46] M. L. W. Basso and J. Maziero, The effect of stationary axisymmetric spacetimes in interferometric visibility, *Gen. Relativ. Gravit.* **53**, 70 (2021).

[47] J. Nemirovsky, E. Cohen, and I. Kaminer, Spin-spacetime censorship, *Ann. Phys.* **534**, 2100348 (2022).

[48] L. Silberstein, *The Theory of Relativity* (Macmillan, London, UK, 1914).

[49] L. H. Thomas, The motion of the spinning electron, *Nature* **117**, 514 (1926).

[50] E. Wigner, On unitary representations of the inhomogeneous Lorentz group, *Ann. Math.* **, 149** (1939).

[51] M. Czachor, Einstein-Podolsky-Rosen-Bohm experiment with relativistic massive particles, *Phys. Rev. A* **55**, 72 (1997).

[52] R. M. Gingrich and C. Adami, Quantum entanglement of moving bodies, *Phys. Rev. Lett.* **89**, 270402 (2002).

[53] A. Peres, P. F. Scudo, and D. R. Terno, Quantum entropy and special relativity, *Phys. Rev. Lett.* **88**, 230402 (2002).

[54] H. Terashima and M. Ueda, Relativistic Einstein-Podolsky-Rosen correlation and Bell’s inequality, *Int. J. Quantum Inf.* **1**, 93 (2003).

[55] A. Peres and D. R. Terno, Quantum information and relativity theory, *Rev. Mod. Phys.* **76**, 93 (2004).

[56] L. Lamata, M. A. Martin-Delgado, and E. Solano, Relativity and Lorentz invariance of entanglement distillability, *Phys. Rev. Lett.* **97**, 250502 (2006).

[57] M. L. W. Basso and J. Maziero, Complete complementarity relations in curved spacetimes, *Phys. Rev. A* **103**, 032210 (2021).

[58] M. L. W. Basso and J. Maziero, Complete complementarity relations and their Lorentz invariance, *Proc. R. Soc. A* **477**, 20210058 (2021).

[59] M. L. W. Basso and J. Maziero, Complete complementarity relations: Connections with Einstein-Podolsky-Rosen realism and decoherence, and extension to mixed quantum states, *Europhys. Lett.* **135**, 60002 (2021).

[60] J. A. Wheeler, The “past” and the “delayed-choice” double-slit experiment, in *Mathematical Foundations of Quantum Theory*, edited by A. R. Marlow (Academic Press, New Orleans, LA, 1978) pp. 9–48.

[61] J. A. Wheeler, Law without law, in *Quantum theory and measurement*, edited by J. A. Wheeler and W. H. Zurek (Princeton University Press, Princeton, NJ, 1983) pp. 182–213.

[62] G. Adesso and D. Girolami, Wave-particle superposition, *Nat. Photonics* **6**, 579 (2012).

[63] R. Auccaise, R. M. Serra, J. G. Filgueiras, R. S. Sarthour, I. S. Oliveira, and L. C. Céleri, Experimental analysis of the quantum complementarity principle, *Phys. Rev. A* **85**, 032121 (2012).

[64] S. S. Roy, A. Shukla, and T. S. Mahesh, NMR implementation of a quantum delayed-choice experiment, *Phys. Rev. A* **85**, 022109 (2012).

[65] A. Peruzzo, P. Shadbolt, N. Brunner, S. Popescu, and J. L. O’Brien, A quantum delayed-choice experiment, *Science* **338**, 634 (2012).

[66] F. Kaiser, T. Coudreau, P. Milman, D. B. Ostrowsky, and S. Tanzilli, Entanglement-enabled delayed-choice experiment, *Science* **338**, 637 (2012).

[67] P. J. Coles, J. Kaniewski, and S. Wehner, Equivalence of wave-particle duality to entropic uncertainty, *Nat. Commun.* **5**, 5814 (2014).

[68] R. Chaves, G. B. Lemos, and J. Pienaar, Causal modeling the delayed-choice experiment, *Phys. Rev. Lett.* **120**, 190401 (2018).

[69] A. L. O. Bilobran and R. M. Angelo, A measure of physical reality, *Europhys. Lett.* **112**, 40005 (2015).

[70] M. Lanzagorta, *Quantum Information in Gravitational Fields* (Morgan & Claypool, San Rafael, CA, 2014).

[71] R. M. Wald, *General Relativity* (University of Chicago Press, Chicago, IL, 1984).

[72] M. Nakahara, *Geometry, Topology and Physics* (Institute of Physics Publishing, Bristol, UK, 1990).

[73] S. Chandrasekhar, *The Mathematical Theory of Black Holes* (Oxford University Press, New York, NY, 1983).

[74] P. M. Alsing, G. J. Stephenson Jr, and P. Kilian, Spin-induced non-geodesic motion, gyroscopic precession, Wigner rotation and EPR correlations of massive spin 1/2 particles in a gravitational field, *arXiv:0902.1396* (2009).

[75] D. N. Page and W. K. Wootters, Evolution without evolution: Dynamics described by stationary observables, *Phys. Rev. D* **27**, 2885 (1983).

[76] A. R. H. Smith and M. Ahmadi, Quantizing time: interacting clocks and systems, *Quantum* **3**, 160 (2019).

[77] N. L. Diaz and R. Rossignoli, History state formalism for Dirac’s theory, *Phys. Rev. D* **99**, 045008 (2019).

[78] E. Castro-Ruiz, F. Giacomini, A. Belenchia, and Č. Brukner, Quantum clocks and the temporal localizability of events in the presence of gravitating quantum systems, *Nat. Commun.* **11**, 2672 (2020).

[79] A. R. H. Smith and M. Ahmadi, Quantum clocks observe classical and quantum time dilation, *Nat. Commun.* **11**, 5360 (2020).

[80] F. Giacomini, Spacetime quantum reference frames and superpositions of proper times, *Quantum* **5**, 508 (2021).

[81] A. Singh, Quantum space, quantum time, and relativistic quantum mechanics, *Quantum Stud. Math. Found.* **9**, 35 (2021).

[82] I. L. Paiva, A. Te’eni, B. Y. Peled, E. Cohen, and

Y. Aharonov, Non-inertial quantum clock frames lead to non-Hermitian dynamics, *Commun. Phys.* **5**, 298 (2022).

[83] T. Favalli and A. Smerzi, A model of quantum spacetime, *AVS Quantum Sci.* **4**, 044403 (2022).

[84] P. Busch, M. Grabowski, and P. J. Lahti, *Operational quantum physics*, Lecture Notes in Physics Monographs, Vol. 31 (Springer, 1995).

[85] P. A. Höhn, A. R. H. Smith, and M. P. E. Lock, Trinity of relational quantum dynamics, *Phys. Rev. D* **104**, 066001 (2021).

[86] K. Lorek, J. Louko, and A. Dragan, Ideal clocks—a convenient fiction, *Class. Quantum Grav.* **32**, 175003 (2015).

[87] M. C. Palmer, M. Takahashi, and H. F. Westman, Localized qubits in curved spacetimes, *Annals of Physics* **327**, 1078 (2012).

[88] B. N. Esfahani, Spin entanglement of two spin-1/2 particles in a classical gravitational field, *J. Phys. A: Math. Theor.* **43**, 455305 (2010).